 CMC, vol.33, no.3, pp.213-228, 2013

Domain Type Kernel-Based Meshless Methods for Solving Wave Equations

L.H. Kuo[1], M.H. Gu[2], D.L. Young[3], C.Y. Lin[3]

Abstract: Coupled with the Houbolt method, a third order finite difference time marching scheme, the method of approximate particular solutions (MAPS) has been applied to solve wave equations. Radial basis function has played an important role in the solution process of the MAPS. To show the effectiveness of the MAPS, we compare the results with the well known Kansa's method, time-marching method of fundamental solutions (TMMFS), and traditional finite element methods. To validate the effectiveness and easiness of the MAPS, four numerical examples which including regular, smooth irregular, and non-smooth domains are given.

Keywords: the method of fundamental solutions, radial basis functions, meshless methods, the method of particular solutions, Houbolt method.

1 Introduction

There were many numerical methods proposed for solving hyperbolic-type partial differential equations such as wave equations which govern many different physical problems. For instance, water wave propagation in water bodies, the stress wave in an elastic solid and sound wave propagation in a medium. But, the development of accurate and efficient numerical methods remains an important and challenging work in the field of scientific computing.

Over the past two decades, many meshless methods have been proposed and widely circulated in the community of science and engineering. In general, the meshless methods can be classified into domain-type and boundary-type methods. The domain-type meshless numerical methods such as the smoothed particle hydrodynamics (SPH) Jiang, Oliveira and Sousa (2007) and the kernel based collocation

[1] Department of Mathematics, University of Southern Mississippi, MS 39406, U.S.A
[2] National Center for Research on Earthquake Engineering , Taiwan
[3] Department of Civil Engineering, National Taiwan University, Taiwan

(KBC) method Kansa (1990a,b) were well developed for solving partial differential equations. The boundary-type meshless methods such as the MFS Fairweather and Karageorghis (1998); Golberg and Chen (1998), the hyper-singular meshless method (HMM) Young, Chen and Lee (2005) and the Trefftz method Chen, Lee, Yu and Shieh (2009); Chen, Liu and Chang (2009); Chen, Wu, Lee and Chen (2007), boundary knot method (BKM) Chen (2002), etc. have also been developed to obtain solutions of homogeneous partial differential equations.

The MFS, a KBC method, was first proposed to approximate the solutions of homogeneous elliptic-type partial differential equations Kupradze and Aleksidze (1964); Mathon and Johnston (1977). Coupled with the use of the method of the particular solutions, the MFS has been extended to solving inhomogeneous partial differential equations Golberg (1995); Golberg and Chen (1998). With the derivation of the particular solution of Helmholtz-type equations using radial basis functions Chen and Rashed (1998), the MFS has further extended to solving various types of time-dependent problems Chen, Golberg and Rashed (1998). Furthermore, the Eulerian-Lagrangian method (ELM) was combined with MFS to deal with the multi-dimensional Burgers and wave equation (called Eulerian-Lagrangian method of fundamental solutions, ELMFS) Gu, Young and Fan (2009); Young, Fan, Hu and Atluri (2008). Moreover, the time-marching method of fundamental solution (TMMFS)has been successfully applied in the wave equations and the result is competitive with the finite element method (FEM) Gu, Fan and Young (2011); Young, Gu and Fan (2008). However, the challenge of choosing the location of source points of the MFS and the uncertainty of determining the shape parameter of radial basis functions have posed difficulties for the TMMFS.

Recently, the method of approximate particular solutions (MAPS) Chen, Fan and Wen (2011, 2012) has been developed by simply applying the particular solution of the given differential operator as the kernel basis without using the MFS. The MAPS is inspired by the work of Sarra Sarra (2006) which showed that the integrated RBFs are more stable and accurate than the regular RBFs. In the numerical implementation, we choose MQ as the kernel basis with good value of shape parameter Rippa (1999); Wertz, Kansa and Ling (2006). The kernel basis for the MAPS is obtained in a similar way as in Sarra (2006) except integrating with respect to the Laplacian. In this paper, we couple the MAPS with the Houbolt method Houbolt (1950); Soroushian and Farjoodi (2008); Wu (2001); Young, Gu and Fan (2008) which is a third order finite difference scheme to solve the wave equations. By the Houbolt method, we reduce the given wave equation to Poisson-type equation. At each time step, the KBC methods such as the MAPS, and the Kansa's method have been applied to solve the Poisson-type equation. The main purpose of this paper is to demonstrate the effectiveness of the MAPS when coupled with the Houbolt

method.

In Section 2, a brief review of the Houbolt method and kernel-based collocation methods are given. In Section 3, four numerical examples with regular and irregular domains are given to illustrate the effectiveness of the kernel-based meshless methods. We also compare the MAPS and the Kansa's method with other traditional methods such as FEM. In Section 4, we make the concluding remarks.

2 Wave Equation

Let Ω be a bounded domain in $\mathbb{R}^2$ with boundary $\partial\Omega = \partial\Omega_D \cup \partial\Omega_N$ and $\partial\Omega_D \cap \partial\Omega_N = \emptyset$. In this paper we consider the following **wave equation**:

$$u_{tt}(\mathbf{x},t) = k^2 \Delta u(\mathbf{x},t) - f(\mathbf{x},t), \qquad \mathbf{x} \in \Omega,\ t > 0, \tag{1}$$

with boundary conditions:

$$\begin{aligned} u(\mathbf{x},t) &= h_D(\mathbf{x},t), \quad \mathbf{x} \in \partial\Omega_D,\ t > 0, \\ \frac{\partial u}{\partial n}(\mathbf{x},t) &= h_N(\mathbf{x},t), \quad \mathbf{x} \in \partial\Omega_N,\ t > 0, \end{aligned} \tag{2}$$

and initial conditions:

$$u(\mathbf{x},0) = I_1(\mathbf{x}), \quad \mathbf{x} \in \Omega, \tag{3}$$

$$u_t(\mathbf{x},0) = I_2(\mathbf{x}), \quad \mathbf{x} \in \Omega, \tag{4}$$

where Δ is the Laplacian, k a constant, t the time variable, n the outward unit vector normal to $\partial\Omega$, and $h_D(\mathbf{x},t)$, $h_N(\mathbf{x},t)$, $I_1(\mathbf{x})$, $I_2(\mathbf{x})$, and $f(\mathbf{x},t)$ are known functions.

Many numerical methods have been developed for solving wave equations. In general, we first try to remove the time dependent varialbe by various numerical schemes. In this paper we focus on the Houbolt method which is a third order time marching scheme to transform the given wave equation to a series of elliptical differential equations.

Houbolt Method

To remove the time variable, the wave equation (1) and its boundary conditions (2) are reformulated as follows:

$$\Delta u(\mathbf{x},t) = \frac{1}{k^2} u_{tt}(\mathbf{x},t) + \frac{1}{k^2} f(\mathbf{x},t), \qquad \mathbf{x} \in \Omega,\ t > 0, \tag{5}$$

$$Bu(\mathbf{x},t) = h(\mathbf{x},t), \qquad \mathbf{x} \in \partial\Omega,\ t > 0, \tag{6}$$

where B is the boundary operator. The time domain of wave equation is discretized by Houbolt finite difference method Houbolt (1950); Soroushian and Farjoodi (2008); Young, Gu and Fan (2008) which required to solve the Taylor series expansions as follows:

$$u^n \approx u^{n+1} - (\delta t)\, u_t^{n+1} + \frac{(\delta t)^2}{2} u_{tt}^{n+1} - \frac{(\delta t)^3}{6} u_{ttt}^{n+1} \tag{7}$$

$$u^{n-1} \approx u^{n+1} - (2\,\delta t)\, u_t^{n+1} + \frac{(2\,\delta t)^2}{2} u_{tt}^{n+1} - \frac{(2\,\delta t)^3}{6} u_{ttt}^{n+1} \tag{8}$$

$$u^{n-2} \approx u^{n+1} - (3\,\delta t)\, u_t^{n+1} + \frac{(3\,\delta t)^2}{2} u_{tt}^{n+1} - \frac{(3\,\delta t)^3}{6} u_{ttt}^{n+1} \tag{9}$$

where $u^n = u(\mathbf{x}, t^n)$, $\delta t = t^{n+1} - t^n$, $u_t^{n+1} = \partial u^{n+1}/\partial t$, $u_{tt}^{n+1} = \partial^2 u^{n+1}/\partial t^2$, and $u_{ttt}^{n+1} = \partial^3 u^{n+1}/\partial t^3$. After solving Eqns. (7), (8), and (9), the Houbolt method can be obtained as follows:

$$u_t^{n+1} \approx \frac{1}{6\,\delta t}(11\,u^{n+1} - 18\,u^n + 9\,u^{n-1} - 2\,u^{n-2}), \tag{10}$$

$$u_{tt}^{n+1} \approx \frac{1}{\delta t^2}(2\,u^{n+1} - 5\,u^n + 4\,u^{n-1} - u^{n-2}). \tag{11}$$

From Eqns. (5) and (6), we have

$$\Delta u^{n+1} - \frac{2}{k^2\,\delta t^2} u^{n+1} = \frac{1}{k^2\,\delta t^2}(-5\,u^n + 4\,u^{n-1} - u^{n-2}) + \frac{1}{k^2} f(\mathbf{x}, t^{n+1}), \qquad \mathbf{x} \in \Omega, \tag{12}$$

$$Bu\left(\mathbf{x}, t^{n+1}\right) = h\left(\mathbf{x}, t^{n+1}\right), \qquad \mathbf{x} \in \partial\Omega. \tag{13}$$

In order to fully implement the Houbolt method, we need to know the initial values of the first three time steps. As a result, the Euler method with very tiny step will be implemented to obtain the initial values of these three time steps. After that, the right hand side of Eqns. (12) and (13) are known and the Houbolt method can be started. Meanwhile, the left hand side of equations are discretized by Kernel based collocation method which is to be described in next section.

Kernel Based Collocation Method

The KBC method (Kernel Based Collocation Method) is one of the well-known meshless methods for solving PDE problems. In this section, we brief review how the method coupled with the time discretization scheme we introduced in the last section for solving wave equations.

Let $\{\mathbf{x}_j\}_{j=1}^{m}$ be m distinct collocation points in $\overline{\Omega}$ of which $\{\mathbf{x}_j\}_{j=1}^{m_i}$ are in Ω and $\{\mathbf{x}_j\}_{j=m_i+1}^{m}$ are in $\partial\Omega$. The main idea of the KBC method is to approximate the exact solution $u(\mathbf{x},t_{n+1})$ at each time step by kernel as follows:

$$\Delta\hat{u}(\mathbf{x},t_{n+1}) = \sum_{j=1}^{m} \alpha_j^{n+1}\,\Delta\Phi(r_j) = \sum_{j=1}^{m} \alpha_j^{n+1}\,\phi(r_j), \tag{14}$$

$$\hat{u}(\mathbf{x},t_{n+1}) = \sum_{j=1}^{m} \alpha_j^{n+1}\,\Phi(r_j), \tag{15}$$

$$\frac{\partial\hat{u}}{\partial n}(\mathbf{x},t_{n+1}) = \sum_{j=1}^{m} \alpha_j^{n+1}\,\frac{\partial\Phi}{\partial n}(r_j), \tag{16}$$

where $r_j = \|\mathbf{x}-\mathbf{x}_j\|,\ j = 1,2,...,m$. Therefore, at each time step Eqns. (12) and (13) can be approximated as follows:

$$\phi_i^{n+1} - \frac{2}{k^2\,\delta t^2}\Phi_i^{n+1} = \frac{1}{k^2\,\delta t^2}(-5\,\Phi^n + 4\,\Phi^{n-1} - \Phi^{n-2}) + \frac{1}{k^2} f(\mathbf{x}_i)^{n+1},\ i = 1,...,m_i \tag{17}$$

$$B\Phi_i^{n+1} = h\left(\mathbf{x}_i, t^{n+1}\right), \qquad i = m_i+1,...,m \tag{18}$$

where

$$\Phi_i^{n+1} = \sum_{j=1}^{m} \alpha_j^{n+1}\Phi(r_{ij}), \qquad r_{ij} = \|\mathbf{x}_i - \mathbf{x}_j\|, \tag{19}$$

$$\phi_i^{n+1} = \sum_{j=1}^{m} \alpha_j^{n+1}\phi(r_{ij}), \qquad r_{ij} = \|\mathbf{x}_i - \mathbf{x}_j\|. \tag{20}$$

The above linear system can be written as the following matrix form:

$$\begin{bmatrix} \phi - \frac{2}{k^2\,\delta t^2}\Phi \\ B\Phi \end{bmatrix}_{m\times m} \begin{bmatrix}\ \alpha^{n+1}\ \end{bmatrix}_{m\times 1} = \begin{bmatrix} \frac{1}{k^2\,\delta t^2}\left[-5\,\Phi^n + 4\,\Phi^{n-1} - \Phi^{n-2}\right] + \frac{1}{k^2} f^{n+1} \\ h \end{bmatrix}_{m\times 1}. \tag{21}$$

where ϕ and Φ for the Kansa's method and the MAPS in the two dimensional case are listed as follows:

The Kansa's method Kansa (1990a,b):

$$\Phi = \sqrt{r^2 + c^2}, \tag{22}$$

$$\phi = \frac{\left(r^2 + 2\,c^2\right)}{\left(\sqrt{r^2 + c^2}\right)^3}. \tag{23}$$

The MAPS Chen, Fan and Wen (2011, 2012):

$$\Phi = \frac{1}{9}\left(r^2+4c^2\right)\left(\sqrt{r^2+c^2}\right) - \frac{c^3}{3}\ln\left(c+\sqrt{r^2+c^2}\right), \tag{24}$$

$$\phi = \sqrt{r^2+c^2}. \tag{25}$$

Note that the $m \times m$ interpolation matrix in Eqn. (21) remains unchange for each time step. Hence, we need only one matrix inversion for all the time steps. As a result, the solution process is very efficient.

The Houbolt method is a third order multi-steps scheme to deal with the time dependent problem. For solving the first two steps Φ^1 and Φ^2, we need the numerical data Φ^0, Φ^{-1}, and Φ^{-2}. Notice that Φ^0 is the given initial condition in Eqn. (3), and the Φ^{-1}, and Φ^{-2} can be obtained using the Euler method associated with initial conditions in Eqns. (3) and (4) as follows:

$$\begin{cases} \Phi^{-1} = I_1(\mathbf{x}) - \delta t \cdot I_2(\mathbf{x}) \\ \Phi^{-2} = I_1(\mathbf{x}) - 2\,\delta t \cdot I_2(\mathbf{x}) \end{cases} \tag{26}$$

3 Numerical results

To demonstrate the efficiency and consistency of the proposed **K**ernel **B**ased **C**ollocation methods, four numerical examples are considered in this section. The examples are examined in the same possible factors which will affect the accuracy. For instance, the numbers of node, the length of the time step, and the shape parameter of MQ. Furthermore, a good shape parameter c of kernel function has to be chosen properly Rippa (1999); Wertz, Kansa and Ling (2006). To validate the numerical accuracy of the solution u, we use the L^2 relative error (E_{L^2}) which is defined as follows:

$$E_{L^2} = \left(\frac{\sum_{j=1}^{m_t} \left(u(x_j) - \hat{u}(x_j)\right)^2}{\sum_{j=1}^{m_t} u^2(x_j)} \right)^{1/2} \tag{27}$$

where the m_t is the number of testing points, u and $\hat{u}$ are exact and approximate solution respectively. The test points are randomly selected. For the notation in all the numerical examples, we denote m as the total number of interpolation points which include the interior and boundary points, m_i the number of interior points, c the shape parameter of MQ.

The computation were performed using MATLAB on a Window 7, 32 bit, Intel Core i7 M520 with 2.5GHz CPU and 4GB memory.

Example 1 In the first example, we consider the wave equation in a unit square as follows:

$$u_{tt}(x,y,t) = \Delta u(x,y,t) + f(x,y,t), \qquad (x,y) \in \Omega,\ t > 0. \tag{28}$$

where

$$f(x,y,t) = (2x(1-x) + 2y(1-y) - x(1-x)y(1-y))\cos(t). \tag{29}$$

The initial and boundary condition are given as follows:

$$u(x,y,0) = 1 + x(1-x)y(1-y), \qquad (x,y) \in \partial\Omega, \tag{30}$$

$$u_t(x,y,0) = 0, \qquad (x,y) \in \partial\Omega, \tag{31}$$

$$u(x,y,t) = x(1-x)y(1-y)\cos(t), \qquad (x,y) \in \Omega. \tag{32}$$

The analytical solution is given as follows:

$$u^*(x,y,t) = 1 + x(1-x)y(1-y)\cos(t). \tag{33}$$

For the numerical implementation, we choose 400 evenly distributed interior and boundary interpolation points in $\overline{\Omega}$ and set the time step $\delta t = 0.02$. In the Figure 1, we show the relative errors E_{L^2} of both methods. No significant difference in term of accuracy has been observed. In Table 1, the maximum relative errors of the MAPS is similar to the Kansa's method when we extended the simulation to a much larger time domain $t \in [0, 100]$.

For the results showed in Figure 1 and Table 1, we observe that the accumulated error which is commonly happen over a long simulation period is apparently not occurred for an extended period of time. This is significant for solving time-dependent problems, in particular for the wave equations. This is an indication that both methods are not only accurate but also stable. In the time-dependent problems, the stability of the computational algorithm is as important as the accuracy and efficiency.

Example 2 In this example, we investigate the homogeneous wave equation in irregular domain which is considered in Gu, Fan and Young (2011). The wave problem can be written as follows:

$$u_{tt}(x,y,t) = \Delta u(x,y,t), \qquad (x,y) \in \Omega,\ t > 0. \tag{34}$$

$$u(x,y,0) = 3, \qquad (x,y) \in \Omega, \tag{35}$$

$$u_t(x,y,0) = \frac{\sqrt{2}\pi}{10}\cos\left(\frac{\pi x}{10}\right)\cos\left(\frac{\pi y}{10}\right), \qquad (x,y) \in \Omega, \tag{36}$$

$$u(x,y,t) = 3 + \cos\left(\frac{\pi x}{10}\right)\cos\left(\frac{\pi y}{10}\right)\sin\left(\frac{\sqrt{2}\pi t}{10}\right), \qquad (x,y) \in \partial\Omega. \tag{37}$$

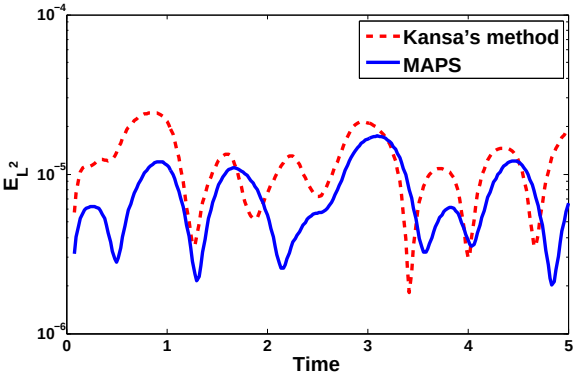

Figure 1: E_{L^2} relative error for $m = 400$ in a unit square in Example 1.

Table 1: Maximum relative error E_{L^2} using various number of interpolation points with time step $\delta t = 0.02$ and $t \in [0, 100]$ in Example 1.

		MAPS		*Kansa*	
m	m_i	c	E_{L^2}	c	E_{L^2}
196	144	0.5	4.4×10^{-5}	0.64	5.5×10^{-5}
289	225	0.37	2.6×10^{-5}	0.47	3.4×10^{-5}
400	324	0.30	1.7×10^{-5}	0.39	2.6×10^{-5}
529	441	0.25	1.4×10^{-5}	0.32	2.5×10^{-5}

The analytical solution is given by

$$u^*(x,y,t) = 3 + \cos\left(\frac{\pi x}{10}\right)\cos\left(\frac{\pi y}{10}\right)\sin\left(\frac{\sqrt{2}\pi t}{10}\right) \tag{38}$$

The irregular domain (see Figure 2) is defined as follows:

$$\partial\Omega = \{(r(\theta)\cos(\theta), r(\theta)\sin(\theta)) : \theta \in [0, 2\pi)\}$$

where

$$r(\theta) = 10\left[\cos(4\theta) + \left(\frac{18}{5} - \sin^2(4\theta)\right)^{1/2}\right]^{1/3}$$

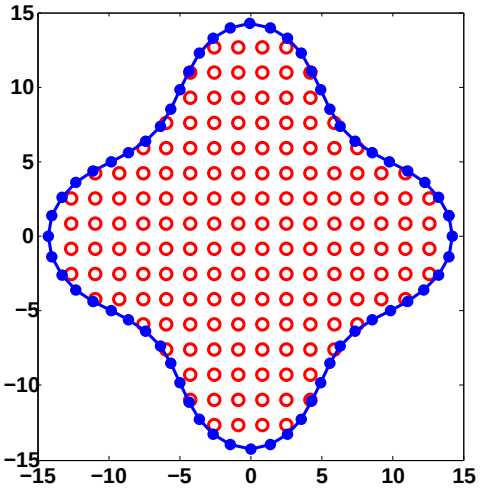

Figure 2: Profile of the computational domain (Cassini) in Example 2.

In the numerical implementation, we choose 400 evenly distributed interior and boundary points in $\overline{\Omega}$ with the time step $\delta t = 0.02$ for both methods. Figure 3 (left) shows that the E_{L^2} error over a long period of time ($t \in [0,120]$). We observe that the errors are stably oscillating between 10^{-5} and 10^{-4} without accumulating the error. In Figure 3 (left) we observe that the error of the MAPS method is half order more accurate than the Kansa's method. In Table 2, we observe that the MAPS requires only $m = 200$ to reach a very high accuracy in a large domain and a long period of time $t \in [0,120]$. The MAPS converges rapidly and hence very efficient. Furthermore, when comparing the results with the MFS-MPS and FEM as shown in Figure 3 (right) Gu, Fan and Young (2011), the MAPS is apparently much superior in term of accuracy and stability. From Table 2, the MAPS is slightly better than the Kansa's method.

Example 3 In this example we consider the same wave equation as in the last example but with more complicate domain and without symmetry. The profile of the domain is shown in Figure 4. The parametric equation of the boundary of the domain is as follows:

$$\partial\Omega = \{(r(\theta)\cos(\theta), r(\theta)\sin(\theta)) : \theta \in [0, 2\pi)\}$$

where

$$r(\theta) = e^{\sin(\theta)}\sin^2(2\theta) + e^{\cos(\theta)}\cos^2(2\theta).$$

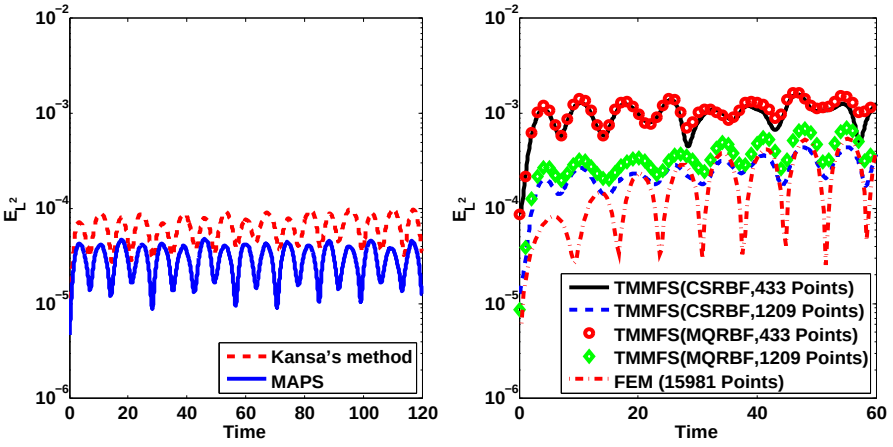

Figure 3: E_{L^2} relative error using $m = 400$ (left) and the results obtained in Gu, Fan and Young (2011).

Table 2: Maximum relative error E_{L^2} using $\delta t = 0.02$ with time domain $t \in [0, 120]$ in Example 2.

		MAPS		*Kansa*	
m	m_i	c	E_{L^2}	c	E_{L^2}
200	136	6.8	4.5×10^{-5}	9.0	1.4×10^{-4}
300	205	5.3	4.4×10^{-5}	7.6	7.0×10^{-5}
400	268	2.8	4.8×10^{-5}	3.9	9.9×10^{-5}
500	328	2.3	6.9×10^{-5}	3.8	9.8×10^{-5}
1400	976	1.3	5.5×10^{-5}	2.1	1.2×10^{-4}

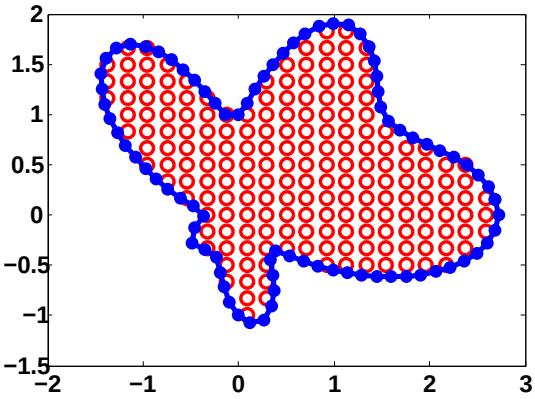

Figure 4: The profile of computational domain (Amoeba) in Example 3.

In the numerical implementation, we choose $\delta t = 0.02$ for the Houbolt method. In general, the error will oscillate when time goes by for wave equation. But in the case, Figure 5 shows that the error is coincidentally stable in the time domain $t \in [0, 120]$. In Table 3, we observe that the MAPS is slightly more accurate than the Kansa's method. Both methods converge rapidly to its potential. Therefore, the numerical error for the the MAPS is more stable and a half order more accurate than the Kansa's method in this example of irregular domain.

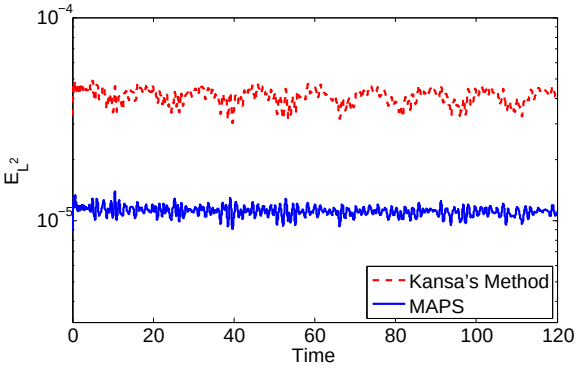

Figure 5: E_{L^2} relative error for $m = 400$ in Example 3.

Table 3: Maximum E_{L^2} relative error. Time step $\delta t = 0.02$, with time domain $t \in [0, 120]$ in Example 3.

		MAPS		*Kansa*	
m	m_i	c	E_{L^2}	c	E_{L^2}
100	64	0.05	4.6×10^{-4}	0.21	1.6×10^{-3}
200	145	0.1	1.5×10^{-4}	0.19	4.8×10^{-4}
300	237	0.12	1.0×10^{-4}	0.25	3.3×10^{-4}
400	317	0.22	1.4×10^{-5}	0.35	4.9×10^{-5}

Example 4 In this example, we consider the following wave equation

$$u_{tt}(x,y,t) = \Delta u(x,y,t), \qquad (x,y) \in \Omega,\ t > 0 \tag{39}$$

$$u(x,y,0) = 2 + \sin(\frac{\pi x}{4}) \sin(\frac{\pi y}{4}), \qquad (x,y) \in \Omega, \tag{40}$$

$$u_t(x,y,0) = 0, \qquad (x,y) \in \Omega, \tag{41}$$

$$u(x,y,t) = 2, \qquad (x,y) \in \partial\Omega, \tag{42}$$

where Ω is a L shape domain (see Figure 6). The analytical solution is given as follows:

$$u^*(x,y,t) = 2 + \sin(\frac{\pi x}{4}) \sin(\frac{\pi y}{4}) \cos(\frac{\sqrt{2}\pi t}{4}) \tag{43}$$

In this example, we intend to test the effectiveness of both methods for the non-smooth and irregular domain. For the numerical implementation, we choose $\delta t = 0.02$ for the Houbolt method for $t \in [0, 120]$. In Figure 7, we choose $m = 408$ for both the Kansa's method and the MAPS which has the clear advantage with respect to the FEM. The Figure 7 and the Table 4 are the results of the Kansa's, MAPS, and FEM methods. In Table 4, we observe that the MAPS requires only $m = 225$ to reach the accuracy of 10^{-4} while the Kansa's method requires $m = 408$ to have such accuracy. For the FEM, the convergent rate is much slower. The MAPS has the clear advantages in term of accuracy, convergent rate, and stability.

4 Conclusion

In this study, the solution of wave equations are approximated by two domain type kernel-based collocation meshless methods (the Kansa's and MAPS methods). In

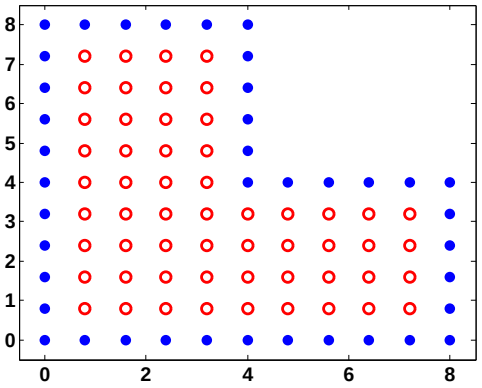

Figure 6: The profile of the non-smooth Domain - L shape.

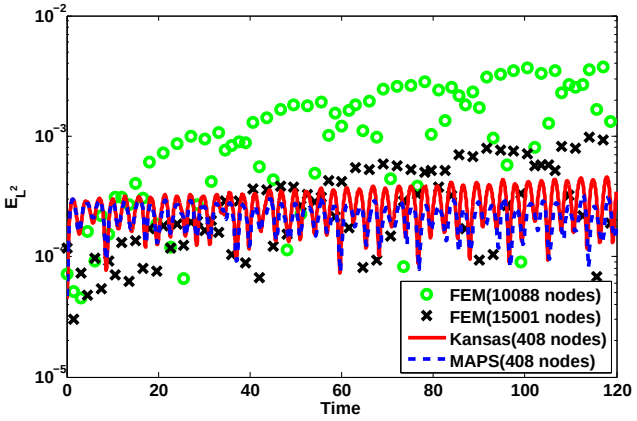

Figure 7: E_{L^2} relative error for $m = 408$ in Example 4.

Table 4: E_{L^2} relative error. The time step $\delta t = 0.02$ with time domain $t \in [0, 120]$ for the MAPS, the Kansa's method, and FEM in Example 4.

		MAPS		*Kansa*		*FEM*	
m	m_i	c	E_{L^2}	c	E_{L^2}	m	E_{L^2}
96	56	3.3	1.5×10^{-2}	4.2	2.9×10^{-2}	1027	2.2×10^{-2}
225	161	2.1	4.1×10^{-4}	2.95	1.9×10^{-3}	5004	2.6×10^{-3}
408	320	1.28	3.3×10^{-4}	2.1	4.6×10^{-4}	10088	1.8×10^{-4}
736	616	0.68	2.9×10^{-4}	1.35	3.0×10^{-4}	15001	3.5×10^{-4}

addition, the standard Houbolt method is implemented to remove the time variable. The numerical results show that the MAPS is superior to the Kansa's method in term of accuracy and stability. The superiority of the MAPS is even more pronouncing for the case of non-smooth and irregular boundary. Comparing to other numerical methods such as TMMFS or FEM, both the Kansa's method and MAPS have clear advantages in term of accuracy and stability.

Acknowledgement

The second author would like to acknowledge the support of the NARL of Taiwan under the grant of 060101A9920. The third author would like to acknowledge the support of the NSC of Taiwan under the grant of NSC100-2221-E-002-020.

References

Chen, C.; Fan, C.; Wen, P. (2011): The method of particular solutions for solving elliptic problems with variable coefficients. *The International Journal for Numerical Methods in Biomedical Engineering*, vol. 8, pp. 545–559.

Chen, C.; Fan, C.; Wen, P. (2012): The method of particular solutions for solving certain partial differential equations. *Numerical Methods for Partial Differential Equations*, vol. 28, pp. 506–522. doi: 10.1002/num.20631.

Chen, C.; Golberg, M.; Rashed, Y. (1998): A mesh free method for linear diffusion equations. *Numerical Heat Transfer, Part B*, vol. 33, pp. 469–486.

Chen, C.; Rashed, Y. (1998): Evaluation of thin plate spline based particular solutions for Helmholtz-type operators for the DRM. *Mech. Res. Comm.*, vol. 25, pp. 195–201.

Chen, J.; Lee, Y.; Yu, S.; Shieh, S. (2009): Equivalence between the trefftz method and the method of fundamental solution for the annular green's function using the addition theorem and image concept. *Engineering Analysis with Boundary Elements*, vol. 33, no. 5, pp. 678–688.

Chen, J.; Wu, C.; Lee, Y.; Chen, K. (2007): On the equivalence of the trefftz method and method of fundamental solutions for laplace and biharmonic equations. *Computers and Mathematics with Applications*, vol. 53, no. 6, pp. 851–879.

Chen, W. (2002): Symmetric boundary knot method. *Engineering Analysis with Boundary Elements*, vol. 26, pp. 489–494.

Chen, Y.; Liu, C.; Chang, J. (2009): Applications of the modified trefftz method for the laplace equation. *Engineering Analysis with Boundary Elements*, vol. 33, no. 2, pp. 137–146.

Fairweather, G.; Karageorghis, A. (1998): The method of fundamental solution for elliptic boundary value problems. *Advances in Computatonal Mathematics*, vol. 9, pp. 69–95.

Golberg, M. (1995): The method of fundamental solutions for poisson's equations. *Engineering Analysis with Boundary Elements*, vol. 16, no. 3, pp. 205–213.

Golberg, M.; Chen, C. (1998): The method of fundamental solutions for potential, Helmholtz and diffusion problems. In Golberg, M.(Ed): *Boundary Integral Methods: Numerical and Mathematical Aspects*, pp. 103–176. WIT Press.

Gu, M.; Fan, C.; Young, D. (2011): The method of fundamental solutions for the multi-dimensional wave equations. *Journal of Marine Science and Technology*, vol. 19, no. 6, pp. 586–595.

Gu, M.; Young, D.; Fan, C. (2009): The method of fundamental solutions for one-dimensional wave equations. *CMC: Computers, Materials & Continua*, vol. 11, no. 3, pp. 185–208.

Houbolt, J. (1950): A recurrence matrix solution for the dynamic response of elastic aircraft. *Journal of the Aeronautical Sciences*, vol. 17, pp. 540–550.

Jiang, F.; Oliveira, M. S.; Sousa, A. C. (2007): Mesoscale sph modeling of fluid flow in isotropic porous media. *Computer Physics Communications*, vol. 176, pp. 471–480.

Kansa, E. (1990): Multiquadrics - a scattered data approximation scheme with applications to computational fluid dynamics - I. *Comput. Math. Applic.*, vol. 19, no. 8/9, pp. 127–145.

Kansa, E. (1990): Multiquadrics - a scattered data approximation scheme with applications to computational fluid dynamics - II. *Comput. Math. Applic.*, vol. 19, no. 8/9, pp. 147–161.

Kupradze, V.; Aleksidze, M. (1964): The method of functional equations for the approximate solution of certain boundary value problems. *U.S.S.R. Computational Mathematics and Mathematical Physics*, vol. 4, pp. 82–126.

Mathon, R.; Johnston, R. (1977): The approximate solution of elliptic boundary-value problems by fundamental solutions. *SIAM J. Numer. Anal.*, vol. 14, pp. 638–650.

Rippa, S. (1999): An algorithm for selecting a good value for the parameter c in radial basis function interpolation. *Advances in Computational Mathematics*, vol. 11, pp. 193–210.

Sarra, S. A. (2006): Integrated multiquadric radial basis function approximation methods. *Comput. Math. Appl.*, vol. 51, pp. 1283–1296.

Soroushian, A.; Farjoodi, J. (2008): A unified starting procedure for the houbolt method. *Communications in Numerical Methods in Engineering*, vol. 24, no. 1, pp. 1–13.

Wertz, J.; Kansa, E.; Ling, L. (2006): The role of the multiquadric shape parameters in solving elliptic partial differential equations. *Comput. Math. Appl.*, vol. 51(8), pp. 1335–1348.

Wu, T. Y. (2001): *A Study on Time-Discontinuous Galerkin Finite Element Method for Elastodynamic Problems*. PhD thesis, Chung Yuan Christian University, Chung Li, Taiwan, 2001.

Young, D.; Chen, K.; Lee, C. (2005): Novel meshless method for solving the potential problems with arbitrary domain. *Journal of Computational Physics*, vol. 209, no. 1, pp. 290–321.

Young, D.; Fan, C.; Hu, S.; Atluri, S. (2008): The eulerian-lagrangian method of fundamental solutions for two-dimensional unsteady burgers' equations. *Engineering Analysis with Boundary Elements*, vol. 32, no. 5, pp. 395 – 412.

Young, D.; Gu, M.; Fan, C. (2008): The time-marching method of fundamental solutions for wave equations. *Engineering Analysis with Boundary Elements*, vol. 33, no. 12, pp. 1411–1425.